STATISTICAL NANOINDENTATION ANALYSIS OF MODERN DENTAL COMPOSITES

by

Shauna D. Jones, DDS

CPT, DC, USA

Thesis submitted to the Faculty of the
Advanced Education in General Dentistry 2-Year Graduate Program as supported by the
Uniformed Services University of the Health Sciences
In partial fulfillment of the requirements for the degree of
Masters of Oral Biology 2019

UNIFORMED SERVICES UNIVERSITY OF THE HEALTH SCIENCES
POSTGRADUATE DENTAL COLLEGE
SOUTHERN REGION OFFICE
2787 WINFIELD SCOTT ROAD, SUITE 220
JBSA FORT SAM HOUSTON, TEXAS 78234-7510
https://www.usuhs.edu/pdc

THESIS APPROVAL PAGE FOR MASTER OF SCIENCE IN ORAL BIOLOGY

Title of Thesis: "Statistical Nanoindentation Analysis of Modern Dental Composites"

Name of Candidate: Shauna D. Jones
Master of Science Degree
May 21, 2019

THESIS/MANUSCRIPT APPROVED: DATE:

[redacted]

05/21/2019

William J. Greenwood, COL, DC
DEAN, FORT HOOD AEGD 2-YR RESIDENCY
Committee Chairperson

[redacted]

05/21/2019

Michael Mansell, LTC, DC
DIRECTOR FORT HOOD AEGD 2-YR RESIDENCY
Committee Chairperson

[redacted]

05/21/2019

John D. King
ASSISTANT DIRECTOR FORT HOOD AEGD 2-YR RESIDENCY
Committee Member

The author hereby certifies that the use of any copyrighted material in the thesis/ dissertation manuscript entitled:

"Statistical Nanoindentation Analysis of Modern Dental Composites"

is appropriately acknowledged and, beyond brief excerpts, is with the permission of the copyright owner.

[redacted]

Shauna D. Jones
Fort Hood AEGD 2-YR Residency
Uniformed Services University
05/21/2019

Distribution Statement

Distribution A: Public Release.

The views presented here are those of the author and are not to be construed as official or reflecting the views of the Uniformed Services University of the Health Sciences, the Department of Defense or the U.S. Government.

ACKNOWLEDGMENTS

I would like to acknowledge Lt. Col. Wen Lien, who offered guidance throughout the process of conducting this study, and the support of United States Airforce Dental Research and Consultation Service for use of dental testing equipment, as well as providing the materials used in this study.

LTC(P) Michael Mansell and the DHA of the United States Army, who supported the project by providing the materials used in this study and offering guidance throughout the duration of the study.

MAJ Drew Krena, United States Army, who offered editing services.

COPYRIGHT STATEMENT

The author hereby certifies that the use of any copyrighted material in the thesis manuscript entitled: Statistical Nanoindentation Analysis of Modern Dental Composites is appropriately acknowledged and, beyond brief excerpts, is with the permission of the copyright owner.

Shauna D. Jones

May 14, 2019

DISCLAIMER

The views presented here are those of the author and are not to be construed as official or reflecting the views of the Uniformed Services University of the Health Sciences, the Department of Defense or the U.S. Government.

ABSTRACT

Statistical nanoindentation analysis of modern dental composites

CPT Shauna D. Jones, DDS, 2019

Thesis directed by: LTC(P) Michael R. Mansell, Director, Advanced Education in General Dentistry 2-Year Program, Ft. Hood, TX

Introduction: All modern dental composites are designed with two phases, filler and matrix, from where their load-bearing attribute usually arrives from the fillers. However, most would agree the link between filler-matrix features, microstructures, and physical properties for these materials are not well understood. **Objective:** The purpose of this study is to characterize various commercial composites in accordance with their micromechanical properties and microstructural features with a specific focus on the filler-matrix relationship. **Materials and Methods:** Twenty composite brands were tested to determine their microstructural features and micromechanical properties such as elastic modulus (EM), stiffness (S), and hardness (H). EM, S, and H were measured using a nanoindenter with a Berkovich diamond indenter. Five rectangular samples ($2.75x5x12mm^3$) per composite brand were prepared, fixed in epoxy resin, and underwent multiple iterations of polishing, ultimately finishing with 0.25μm polished surfaces. All specimens were stored in 37°C distilled water for 24 hours prior to testing. An indentation load of 10mN was applied (Poisson's ratio = 0.3), and 2000 indents per composite brand

were measured. Microstructural features were analyzed by scanning electron microscopy and laser diffraction particle size analyzer. Data were analyzed with ANOVA/Tukey (α=0.01), t-test, and regression. **Results:** Composite filler sizes exhibited unimodal, bimodal, and multimodal distributions. Bimodal filler distribution responded with significantly higher modulus, hardness, and stiffness than unimodal and multimodal distributions. Additionally, the twenty RBCs were classified based on current terminology, and significant differences ($p<0.01$) in modulus and stiffness were found – rankings in descending order were: Nanohybrids > Hybrids > Microfills. However, hardness rankings showed: Hybrids > Nanohybrids > Microfills. Bivariate regression analyses demonstrated filler weight correlated with modulus with the highest r^2 (0.634), followed by stiffness (r^2=0.625), and then hardness (r^2=0.522). **Conclusion:** Composite systems adopted with new polymeric matrix chemistry behaved differently than methacrylate-based systems ($p<0.01$). In general, filler weight values directly correlated with elastic modulus, hardness, and stiffness.

TABLE OF CONTENTS

INTRODUCTION

Since their advent, resin-based composite (RBCs) restorations have gained popularity both with the general public and dental practitioners. With an esthetically-conscious patient, RBCs have become an attractive treatment option to amalgam and indirect metal-alloy restorations for patients with various restorative needs. Additionally, with the improvement in resin matrix chemistry and nano-particulate formulation, the physical properties and clinical longevity of modern RBCs are rivaling those of traditional amalgam restorations.[1-3]

The evidence-based benefits of RBCs include enabling the practitioner a direct treatment approach to restore form and function of a diseased or injured tooth, allowing a more conservative cavity design and minimally invasive preparation by removing less natural tooth structure, and offering a great scope for variations in esthetics. Nonetheless, there are several disadvantages to consider when deciding whether to restore with RBCs. One particular concern is the potential of a restoration to fail in high stress-bearing areas. The failure of RBC restorations has been extensively investigated, in both clinical and laboratory settings.

Long-term prospective studies and meta-analyses have shown that the most common reasons for RBC failure in the posterior dentition are due to fracture, marginal defects, and secondary caries.[4,5] RBCs may also fail as a result mechanical wear, water sorption on a microscopic scale, and marginal and bulk extrinsic staining/discoloration. Additionally, if the patient cannot tolerate post-operative sensitivity secondary to placement of the restoration, it may be determined to be a failed restoration.[6] Failure by

fracture of the RBC, marginal defects, and mechanical wear may be considered on a macroscopic scale. Of great importance to composite manufacturers and researchers is understanding why these materials fail on a microscopic level, with an aim to determine any possible correlation with microscopic failure and bulk, macroscopic failures.

Contemporary RBCs consist of three main constituents: molecules for initiating polymerization, an organic polymeric matrix, and inorganic filler reinforcements. The filler system is commonly made of inorganic silicon compounds such as silicon dioxide (glass), borosilicates, or lithium aluminum silicates. The inorganic filler is often coated with bipolar molecules (organosilanes) that act as coupling agents to bond interfacially between the fillers and the polymeric matrix. These particulates can be discretely dispersed or colloidally suspended, forming amorphous aggregates, in a non-aqueous, organic medium.[7]

A common categorization of modern RBCs is based on filler size and distribution, with respect to presence of nano-sized and micron-sized inorganic fillers. Further, filler content and morphology allows for improved subcategorization of RBCs. Examples of RBCs based on filler content include microfills, nanofills, microhybrids, and nanohybrids.[8] A challenge arises in describing RBCs solely by their filler size distribution because although a RBC may be categorized as nanohybrid, the content of filler may include varying amounts of filler particles sized larger than 1 micron and may affect the mechanical properties between different RBCs marketed as "nanohybrids".[8] For example, a study by Lohbauer *et al.* determined with *in vitro* testing that commercially marketed nano-filled hybrid RBCs did not yield similar, statistically significant, values with respect to

some of the RBC's physical properties (fracture strength and cyclic flexural fatigue, in particular). The authors advised that although a RBC may be marketed in a particular subcategory, the categorization would not provide a direct correlation to expected outcomes of laboratory mechanical property testing.[9]

Three particularly important mechanical properties may be affected by altering compositions of both filler and matrix chemistry: stiffness, hardness, and elastic modulus. It is of great importance, especially when restoring posterior teeth, that the material mimic the elastic modulus of the supporting structure (i.e. enamel and dentin) and to have an appropriate stiffness and hardness to resist mechanical wear[10]. By definition, the elastic modulus describes the stress and strain relationship on a material under a given load[11]. As a resin-based restoration experiences variable forces throughout the duration of its lifespan, the material will be required to sustain a certain amount of flexure without permanent deformation as varying loads are applied. Ideally, this material will exhibit similar elastic moduli to the supporting tooth structure adjacent to the restoration, with the goal of preventing microleakage, recurrent decay, or dislodgement of the restoration.[12,13] It has been seen in past studies that a positive correlation exists between elastic modulus and filler content.[14]

As can be seen in architectural and even in biological settings, the strength of a structure can be improved by reinforcing with smaller, higher-order substructures. For instance, human bone is hollow but derives its strength from a laminate of fibers woven together. Further, on a microscopic level, the fibers of bone are interwoven with minerals and proteins, which serve to add additional reinforcement. A structure with a small grain

size and larger interface area will be stronger and more fracture resistant. Additionally, materials having these higher-order substructures will likely possess a superplastic quality, which allows the deformation of the material without fracture.[15] With respect to RBCs, the inorganic micro and nano-sized fillers act as the "small grains" and serve as reinforcement for the composite system. In addition to their size, the shape of the filler may affect certain mechanical properties of the RBC. Masouras *et al*. determined a statistically significant difference in modulus of elasticity in RBCs based on filler shape, with irregular filler shapes yielding statistically significant higher elastic modulus values than spherical filler shapes when filler volume was controlled for.[16]

When evaluating the hardness of a material on a macroscopic level, the hardness may be described as a mean pressure the given material will support under an applied load.[17] The significance of hardness, as it relates to dental resin-based composites, is the ability of the material to maintain its original form after the application of a load without permanent deformation. This is especially important, as the restoration may be at greater risk for failure if it becomes permanently deformed due to marginal microleakage and crack propagation. To gain a better understanding of why restorations fail on a macroscopic level, examining hardness on a micro and nanoscopic level has been evaluated. It has been suggested that bulk mechanical properties of materials may differ than properties on a microscopic level because of differences in size effect and surface effect. Quian *et al.* were able to determine that microhardness varied from nanohardness between materials tested in their study, due to the method in which hardness was evaluated.[18]

Classification of modern dental composites based on their filler-matrix attributes is an apparently simple notion. However, most would agree the real complexity is to

understand whether these phases (i.e., filler and matrix) and their varied organization of nano- and micro-structural features are relevant predictors for not only *in vitro* but also *in vivo* performance. Without the reinforcement of a particle phase, the polymeric phase lacks the toughening mechanism, which acts ahead of a crack tip to dissipate its energy and extension. This premise that certain filler attributes are positively correlated with the elastic property of dental composites, enhancing their clinical load-bearing capability, is based on evidences from empirical studies, which relate mechanical strength to clinical wear.[19] However, filler by itself may offer only limited information regarding the bulk properties of dental composites.

Other than describing filler content, morphology, distribution, etc., resin matrix properties may be used to differentiate between RBCs. Dimethacrylates such as BisGMA (bisphenol-A glycidyl methacrylate), UDMA (urethane dimethacrylate) and BisEMA (ethoxylated bisphenol-A glycidyl methacrylate) co-polymerize with a diluent, such as TEGDMA (triethyleneglycol dimethacrylate), to form high degree covalent bonds between methacrylate groups. A matrix with high molecular weight monomers will have less carbon double bonds, thus reducing mobility and rearrangement after polymerization.[20] The advantage translates into reduced polymerization shrinkage. In one study, Kleverlaan and Feilzer described the relationship between unpolymerized resin content and the amount of shrinkage, contraction stress, and tensile modules and ascertained that a lower degree of total polymerization had beneficial effect on reducing the shrinkage and contraction stress properties of a matrix. Thus, an aim of many manufactuers has been a shift to modifiy resin matrix formulations change to combat polymerization shrinkage issues.[21]

Relatively little is known about the effect of elastic-constant mismatch and interfacial bonding interaction between the filler and matrix phases on the micro-crack deflection and macro-performance of dental composites. Furthermore, the relationship between filler-matrix structural features and mechanical performance at various length scales is still an enigma. In this study, a novel, statistical grid nanoindentation approach[22], is applied to investigate the effect of the spatial distribution of fillers' modulus, hardness, and stiffness in relation with the matrix phase. The hypothesis is that resin-based composites with matrices of predominantly methacrylate-based chemistry will behave differently with respect to their stiffness, hardness, and elastic moduli than those with non-methacrylate-based resin matrices. Additionally, it is hypothesized there will be a significant difference between filler composite class types (microfill, nanohybrid, and hybrid), filler shape (irregular, irregular), and filler distribution (unimodal, bimodal, multimodal)with respect to stiffness, hardness, and moduli The null hypotheses are that there will be no difference in behavior of the different RBCs with methacrylate and non-methacrylate-based resin matrices as well as no significant differences of the respective mechanical properties based on composite class type, filler shape, and filler distribution.

MATERIALS AND METHODS

See Table 1 for comprehensive list of RBCs and specifications. Samples for nanoindentation testing were prepared as follows: (1) The fragments obtained from the fracture toughness test or the three-point flexural test (n = 5 per RBC brand) were randomly selected and mounted in a plastic-ring form (Ø = 31.75 mm, Buehler, Lake Bluff, IL, USA) filled with epoxy mounting resins (EpoxiCureTM, Buehler, Lake Bluff, IL, USA).

(2) After 24 hours for allowing the epoxy resins to completely cure, the side of each "puck" that contained the surfaces of the 5 fragments was polished under running water at 200 rpm on a polishing machine (Ecomet 6, Buehler, Lake Bluff, IL, USA): first using silicon carbide paper of 800-, 1000-, and 1200-grit paper (CarbiMetTM, Buehler, Lake Bluff, IL, USA), and then using a MicroClothTM (Buehler, Lake Bluff, IL, USA) along with water-based polycrystalline diamond suspensions of 1, 0.5, and 0.25 μm.

(3) Specimens were ultrasonically cleaned in deionized water using an ultrasonic bath (Ultramet 2002, Buehler, Lake Bluff, IL, USA) for 3 minutes, followed by thorough rinsing with acetone (>99.5% ACS reagent grade, Sigma Aldrich, St. Louis, MO, USA) and then deionized water (Milli-Q®, Merck Millipore, Burlington, MA, USA).

(4) The specimens were stored dry, at room temperature, until testing was performed.

A nanoindentation system (iNano®, Nanomechanics Inc., Oak Ridge, TN, USA), equipped with iNano® proprietary software (Nanomechanics Inc., Oak Ridge, TN, USA) and fitted with a tetrahedral Berkovich diamond indenter tip (Serial # TB26961, Micro Star Technologies, Huntsville, TX, USA) of 20 nm radius (nominal angle of 65.3° from the vertical axis), was used to measure all specimens. The load and displacement resolutions of the iNano® system were 3 nN and 0.02 nm, respectively.

All indentation measurements were conducted in accordance to ISO 14577 [23] and at room temperature. Immediately after the thermal drift rate of the instrument diminished below a 0.05 nm/s threshold, indentation commenced. Each indentation cycle was programmed to consist of four chronological stages:

(1) Tip loading proceeded until contact was achieved and continued until target load was reached, using a constant loading rate.

(2) At target or peak load, the force was held constant for a brief dwelling period.

(3) After which, loading was reduced at a constant unloading rate that was equivalent to the loading rate.

Composite (Abbreviation)	Manufacturer	Material Class	Filler Weight (%)	Filler Volume %	Filler Content (size of content)	Type of matrix	Depth of Cure	Curing Time	Curing Wavelength
Activa BioActive (AB)	Pulpdent	RMGIC-like	56%	-	-	Ionic resin maxtrix	4 mm	20 sec	-
Admira Fusion (AF)	Voco	Nano-hybrid	84%	-	Nano, glass ceramic	Ormocer-(SiO2 backbone), no traditional monomers	2.7 mm	20 sec	-
Beautifil Bulk (BB)	Shofu	High Viscosity Giomer (Hybrid)	87.00%	74.50%	S-PRG filler based on fluoroboroalumino silicate	Bis-GMA, UDMA, Bis-MPEPP,TEGDMA	4mm	10 sec	-
Beautifil Bulk Flow (BBF)	Shofu	Low Viscosity Giomer (Hybrid)	72.50%	51%	S-PRG filler based on fluoroboroalumino silicate	Bis-GMA, UDMA, Bis-MPEPP,TEGDMA	4 mm	10 sec	-
Beautifil II (BII)	Shofu	Hybrid/ Giomer	83.30%	69%	0.01um-4.0 um	Bis-GMA, TEGDMA	5.9 mm	20 sec	-
Durafill VS (D)	Kulzer	Microfill	-	66%	Silicon dioxide, 0.02-0.07 um, splinter polymer < 20 um	Bis-GMA, TEDGMA, urethane dimethacrylate	2 mm	20-40 sec	460-470 nm
Epic-TMPT (EPIC)	Parkell	Microfill	-	-	Proprietary	TMPT (proprietary)	-	20-40 sec	-
Filtek One Bulk Fill (F1B)	3M	Bulk Fill nano-hybrid	76.50%	58.50%	20nm Silica, 4-11nm Zirconia, Ytterbium trifluoride 100 nm	AUDMA, AFM, DDDMA, UDMA	5mm	10-20 sec O/B/L	-
Filtek Supreme Ultra (FSU)	3M	Nano-hybrid	78.50%	63.30%	20 nm silica, 4-11 nm zirconia, aggregated zirconia/silica nanoclusters	Bis-GMA, UDMA, TEGDMA, Bis-EMA(6)	2 mm	20 sec	400-500 nm
Kalore (GCK)	GC America	Nano-hybrid	82%	-	400 nm modified strontium glass, 100nm lanthanoid fluoride,16nm dispersed silica (17 um PPFs)	UDMA, dimethacrylate co-monomers, DX-511	2.5mm	20 sec	-
Majesty Posterior (CM)	Clearfil	Nano-hybrid	92%	82%	1.5um glass filler, 20nm alumina microfiller	Bis-GMA, TEGDMA, hydrophobic aromatic dimethacrylate	1.5 mm	20 sec	400-515nm
N'Durance (N'D)	Septodont	Nano-hybrid	80%	65%	40 nm ytterbium fluoride, silanated 500 nm barium glass and 10 nm silica	ethoxylated BisGMA, UDMA and the new dicarbamate dimethacrylate dimer acid	2.5 mm	30 sec	470-480 nm
Point 4 (P4)	Kerr	Microhybrid	76%	57%	0.4 um	Bis-GMA	2 mm	40 sec	-
Renamel (RM)	Cosmedent	Microfill	70%	60%	.04-2um pyrogenic silica acid	Bis-GMA, Bis-EMA	2mm	20-40 sec	400-500nm
Renamel Nano Plus (RNP)	Cosmedent	Nano-hybrid	78%	60%	0.02-0.7um silica, Ba-Al-Fluro borosilica	BDDMA, Bis-GMA, UDMA	2 mm	20-40 sec	400-500 nm
SonicFill 2 (SF2)	Kerr	Bulk Fill Nano-hybrid	81.35%	-	Silica, Barium glass, YbF3, mixed oxides	Dimethacrylates, Bis-GMA, Bis-EMA	5mm	20sec	400-520 nm
Tetric Evo Ceram (TECB)	Ivoclar Vivadent	Nano-hybrid	76.00%	55%	40nm-3um Ba glass, ytterbium trifluoride, mixed oxides	Bis-GMA, Urethane dimethacrylate, Ethoxylated Bis-EMA	2mm	10 sec	400-500nm
TPH Spectra HV (TPH)	Dentsply-Sirona	Nano-hybrid	77.20%	57.00%	Silanated Ba-Br-F-Al silicate and silicon dioxide 1.35 um	urethane modified Bis-GMA, TEGDMA, polymerizable dimethacrylate resin	2 mm	10 sec	470 nm
Venus Diamond (VD)	Kulzer	Nano-hybrid	81%	64%	5nm-20um, Barium aluminum fluoride glass, discreet nanoparticles	TCD-DI-HEA, UDMA	2 mm	20-40 sec	440-480 nm
Venus Diamond Flow (VDF)	Kulzer	Nano-hybrid	65%	41%	0.02 um-5 um Ba-Al-F silicate, YbF3, SiO2	UDMA, EBADMA	2 mm	20 sec	440-480nm

Table 1: Twenty RBC's and respective specifications. Data obtained from manufacturer's site when possible, otherwise, data obtained from tables listed in previous studies.

(4) Unloading ended when the load dropped to 10% of the target or peak load.

The target load, loading rate, and dwell time were set at 50 mN, 2.5 mN/s, and 2s, respectively.

An array of indents (25 indents per RBC brand arranged in a 5 x 5 grid) were imprinted onto the polished surfaces. Each consecutive indent was spaced 30 μm apart from each other to avoid any interference of residual stresses from adjacent imprints.

For each loading-unloading cycle, the sample exhibited deformation that was partially elastic and partly inelastic, forming force–displacement curves (or a hysteresis loop). The curves were used to evaluate the hardness and elastic modulus values of each RBC. For each indent, elastic modulus was calculated using the standard methods of Oliver and Pharr[17], where the unloading force-displacement curve was fitted to the upper 50% of the maximum force with a power-law expression,

$$P=B\ (h-h_f)^m\ ,$$

where P (mN) and h (nm) were ordered pairs of force-displacement data, and B (mN/nmm), h_f (nm), and m (no unit) were best-fit constants. P is the contact force exerted by the indenter onto the sample, and h is the penetrating displacement of the indenter into the sample, relative to the position at which the indenter first contacted the sample's surface. The contact stiffness, S (mN/nm) was analytically differentiated with respect to displacement and evaluated at the maximum displacement,

$$S=\left(\frac{dP}{dh}\right)_{h=h_{max}} = \ (h_{max}-h_f)^{-1}\ .$$

The tip contact area, A_c (nm^2), a function of contact depth, was determined using the depth to area calibration for the Berkovich tip against a fused silica reference

(Nanomechanics Inc., Oak Ridge, TN, USA). The reduced modulus, E_r (GPa), was calculated using the contact stiffness and contact area at maximum load,

$$E_r = \frac{1}{2}\left(\sqrt{\frac{\pi}{A_c}}\right) S\,.$$

The Elastic modulus, E (GPa), per group was computed from E_r using the following expression,

$$E = (1-\nu^2)\left(\frac{1}{E_r} - \frac{1-\nu_i^2}{E_i}\right)^{-1},$$

where ν is the Poisson's ratio of RBC (ν = 0.3 was used for all RBC brands in this study [Masouras et al., 2008]), and ν_i and E_i are the Poisson's ratio (0.07) and elastic modulus (1141 GPa) of the Berkovich indenter, respectively. The nanoindentation hardness, H (GPa), was obtained from the indentation load divided by the projected contact area, A_c (nm^2),

$$H = \frac{P_{max}}{A_c}$$

where P_{max} is the maximum load and A_c is the contact area between the indenter and the sample as described earlier.

RESULTS

SPSS software was used to determine statistical significance of results, including one way ANOVA, t-test, and bivariate regression analysis. All p values were set to $p<0.01$. Statistically significant differences were found between all three mechanical testing modalities with respect to filler shape, filler-matrix system, filler morphology, and matrix chemistry- thus all null hypotheses were rejected.

Stiffness (S)

Statistically significant differences ($p<0.01$) were found between the following groups of RBCs, with ranges of stiffness values from highest to lowest as follows: CM> VD> TECB> BB, BII, GCK> AF, F1B, RNP, N'D > BBF > FSU, P4, TPH > SF2> VDF > EPIC> AB> RM> D. Statistically significant differences ($p<0.01$) were found between composite classes, with stiffness ranging from greatest to lowest values as follows: Nanohybrid > Hybrid > RMGI > Microfill. Statistically significant differences ($p<0.01$) were also found between stiffness values and filler size distribution. Bimodal filler size distribution had the largest stiffness values, with unimodal following, and lastly multimodal filler size distribution had the lowest stiffness values. With respect to matrix chemistry, RBCs with methacrylate-based resin matrices had statistically significant ($p<0.0001$) higher stiffness values than RBCs with non-methacrylate-based resin matrices. **Table 2** outlines stiffness results.

Hardness (H)

Statistically significant differences ($p<0.01$) were found between the following groups of RBCs, with largest stiffness values to lowest stiffness values as follows: CM> SF2> FSU, VD, BII, AF> F1B, BB> TECB, RNP, N'D, BBF, P4, TPH, GCK>RM, EPIC> D, VDF>AB.

Statistically significant differences ($p<0.01$) were found between composite classes, with hardness values ranging from greatest to lowest as follows: Hybrid > Nanohybrid > Microfill > RMGI. This differed from both stiffness and elastic modulus, which showed

Table 2: Stiffness values (mN/nm) by RBC, RBC type, filler size distribution, and matrix type.
N is number of indents, S.D. is standard deviation, Std. Err.(x) is standard error of the mean

RBC	N	Mean (x)	S.D.	Std. Err. (x)
AB	3901	48010	4574.622	73.243179
AF	1981	59084.65	5029.959	113.0114
BB	1943	60907.62	6121.19	138.86712
BBF	3802	57314.34	7984.279	129.48804
BII	1954	60844.63	4355.928	98.541321
CM	1998	77663.46	8445.662	188.94524
D	1992	41441.37	7513.342	168.34044
EPIC	2000	48636.8	6473.977	144.76253
F1B	1996	58767.59	4404.084	98.576939
FSU	1994	55900.5	3443.513	77.115052
GCK	3970	60609.14	3211.164	50.964437
N'D	1982	58309.64	2144.378	48.166993
P4	1996	55491.88	1074.3	24.046127
RM	1970	42949.29	2194.923	49.452259
RNP	1980	58344.29	1518.474	34.125165
SF2	3967	52956.26	7448.096	118.25355
TECB	1976	68053.34	5507.087	123.88778
TPH	1993	55229.2	1774.702	39.75318
VD	1979	72649.07	6845.257	153.87458
VDF	1987	51362.36	2535.894	56.889502
RBC Type	**N**	**Mean (x)**	**S.D.**	**Std. Err. (x)**
Hybrid	15638	58220.7	7919.75	63.332
Microfill	5962	44353.4	6643.97	86.046
Nanohybrid	21860	60777.4	8535.06	57.727
RMGI	3901	48010.0	4574.62	73.243
Mode	**N**	**Mean (x)**	**S.D.**	**Std. Err. (x)**
Bimodal	29649	58736.5	9823.73	57.052
Multimodal	7944	47835.4	8411.34	94.372
Unimodal	9768	58281.0	5778.55	58.468
Matrix Type	**N**	**Mean (x)**	**S.D.**	**Std. Err. (x)**
Methacrylate	15638	58220.7	7919.75	63.332
Non-methacrylate	5962	44353.4	6643.97	86.046

similar trends in ranking by composite class with nanohybrids yielding largest respective values with hybrids yielding the second largest values on average. Statistically significant differences ($p<0.01$) were also found between hardness values and filler size distribution. Bimodal filler size distributions had the largest average hardness values, with unimodal following, and lastly multimodal filler size distribution with the lowest hardness values. This trend was also seen with respect to both stiffness and elastic modulus values. As pertaining to matrix chemistry, RBCs with methacrylate-based resin matrices had statistically significant ($p<0.001$) higher hardness values than RBCs with non-methacrylate-based resin matrices. See **Table 3** for hardness data.

Elastic Modulus (EM)

Statistically significant differences ($p<0.01$) were found between the following groups of RBCs, with values of elastic modulus ranging from greatest to lowest as follows: CM > VD > BII > AF, BB > TECB, FSU, F1B, SF2 > RNP, N'D, GCK > BBF > P4, TPH > EPIC > VDF > RM > AB > D. Statistically significant differences ($p<0.01$) were found between composite classes, with elastic modulus values ranking from greatest to lowest: Nanohybrid > Hybrid > Microfill > RMGI. Statistically significant differences ($p<0.01$) were also found between elastic modulus values and filler size distribution. Compared with both stiffness and hardness, elastic modulus values also trended from greatest to lowest as follows: bimodal > unimodal > multimodal. As with stiffness and hardness, RBCs with methacrylate-based resin matrices had statistically significant ($p<0.0001$) elastic moduli than RBCs with non-methacrylate-based resin matrices. **Table 4** outlines data for EM.

DISCUSSION

Stiffness, hardness, and elastic modulus were determined using the methods as described by Oliver and Pharr.[17] The mechanical properties were also analyzed with respect to resin-matrix type, filler shape, and filler distribution. The data from the aforementioned analyses were provided from an accompanying study (in process of being prepared for publishing) by Wentworth *et al.*, which used scanning electron microscopy to evaluate RBC surfaces of the samples used in this study and describe the shape of fillers for each composite group sample, as well as determine filler weight percentage (wt%) from thermogravimetric analysis and filler distribution by laser particle diffraction.

While some differences were noted in trends between composite class and *S*, *H*, and *EM*, a few trends were consistent with respect to *S*, *H*, and *EM*. With all three mechanical properties, irregular filler shape had statistically significant larger values than spherical filler shape, which agreed with Masouras *et al*[16]. This data does not agree with the results of certain studies, which have suggested there is no significant difference between hardness and filler shape, and more on the contrary that spherical fillers yield higher hardness values, due to the ability of greater filler loading by volume percentage of spherical fillers.[24,25] See **Table 6** for filler shape data.

It must be noted, however, the method of conducting hardness tests vary between studies, as well as selected composite materials, which may explain differences in results.

Table 3: Hardness values (GPa) by RBC, RBC type, filler size distribution, and matrix type.
N is number of indents, S.D. is standard deviation, Std. Err.(x) is standard error of the mean

RBC	N	Mean (x)	S.D.	Std. Err. (x)
AB	3657	0.557118	0.141147	0.002334
AF	1965	1.494199	0.344752	0.0077772
BB	1895	1.385203	0.359717	0.0082633
BBF	3292	1.054578	0.324467	0.0056551
BII	1886	1.51333	0.341311	0.0078592
CM	1864	3.1311	1.103137	0.0255509
D	1979	0.680106	0.090147	0.0020264
EPIC	1985	0.787129	0.0964	0.0021637
F1B	1947	1.423945	0.288203	0.0065315
FSU	1944	1.580643	0.255757	0.0058007
GCK	3940	0.977787	0.151466	0.0024131
N'D	1972	1.057601	0.100498	0.0022631
P4	1988	1.044673	0.086174	0.0019327
RM	1958	0.831655	0.076044	0.0017185
RNP	1981	1.076133	0.14369	0.0032284
SF2	3967	1.959687	1.236679	0.0196348
TECB	1992	1.077721	0.156135	0.0034983
TPH	1982	1.020732	0.090831	0.0020402
VD	1816	1.568563	0.295994	0.0069458
VDF	1974	0.642016	0.087265	0.0019641
RBC Type	**N**	**Mean (x)**	**S.D.**	**Std. Err. (x)**
Hybrid	15020	1.39471	0.776575	0.00634
Microfill	5922	0.76609	0.10854	0.00141
Nanohybrid	21385	1.34798	0.728635	0.00498
RMGI	3657	0.141147	0.141147	0.00233
Mode	**N**	**Mean (x)**	**S.D.**	**Std. Err. (x)**
Bimodal	28870	1.39681	0.854729	0.00503
Multimodal	7894	0.83891	0.165189	0.00186
Unimodal	9220	1.01963	0.224288	0.00234
Matrix Type	**N**	**Mean (x)**	**S.D.**	**Std. Err. (x)**
Methacrylate	34450	1.31894	0.788116	0.00425
Non-methacrylate	11534	0.94603	0.371145	0.00346

Table 4: Modulus values (GPa) by RBC, RBC type, filler size distribution, and matrix type.
N is number of indents, S.D. is standard deviation, Std. Err.(x) is standard error of the mean

RBC	N	Mean (x)	S.D.	Std. Err. (x)
AB	3641	9.190003	1.185987	0.0196548
AF	1978	18.71188	2.402952	0.0540296
BB	1915	18.67123	2.794117	0.0638499
BBF	3351	14.97866	3.015833	0.0520979
BII	1900	19.44416	2.656403	0.0609421
CM	1959	36.46743	7.20256	0.1627308
D	1974	8.685461	1.290881	0.0290544
EPIC	1995	11.05033	1.190907	0.0266628
F1B	1970	18.17203	1.601182	0.0360751
FSU	1971	18.24069	1.378633	0.0310531
GCK	3941	15.46661	1.206516	0.019219
N'D	1980	15.51798	0.999444	0.0224608
P4	1988	14.65916	0.665447	0.0149247
RM	1988	10.10785	0.737703	0.0165453
RNP	1975	15.63438	1.132207	0.0254766
SF2	3921	18.0545	4.967942	0.0793374
TECB	1977	18.30238	2.063258	0.0464034
TPH	1983	14.41291	0.74146	0.0166505
VD	1862	23.95505	2.865947	0.0664169
VDF	1973	10.57517	0.956605	0.0215362
RBC Type	**N**	**Mean (x)**	**S.D.**	**Std. Err. (x)**
Hybrid	15052	17.2077	3.76366	0.03068
Microfill	5957	9.9521	1.46704	0.01901
Nanohybrid	21592	18.3777	7.02414	0.04780
RMGI	3641	9.1900	1.18599	0.01965
Mode	**N**	**Mean (x)**	**S.D.**	**Std. Err. (x)**
Bimodal	29025	17.8559	7.06517	0.04147
Multimodal	7937	11.3406	2.76862	0.03108
Unimodal	9280	15.1174	2.02493	0.02102
Matrix Type	**N**	**Mean (x)**	**S.D.**	**Std. Err. (x)**
Methacrylate	34702	16.8986	6.76887	0.03634
Non-methacrylate	11540	14.0513	3.78614	0.03524

Table 5: Filler Weight (wt%) by RBC brand. ($p<0.01$)

N is number of samples tested by thermogravimetric analysis, S.D. is standard deviation, Std. Err.(x) is standard error of the mean

RBC	N	Mean (x)	S.D.	Std. Err. (x)
AB	2	55.1731	0.47680	0.33710
AF	2	84.8953	1.43133	1.01210
BB	2	74.7137	0.07616	0.05380
BBF	2	68.3999	0.48854	0.34540
BII	2	79.0000	0.09899	0.07000
CM	2	88.9021	0.23052	0.16300
D	2	57.1758	0.16164	0.11430
EPIC	2	46.5900	0.07255	0.05130
F1B	2	71.4274	0.28277	0.20000
FSU	3	72.7999	0.21249	0.1227
GCK	3	69.6494	0.14496	0.0837
N'D	2	75.0018	0.71368	0.50460
P4	2	73.8382	0.00410	0.00290
RM	2	57.5347	0.32633	0.23080
RNP	2	77.9637	0.38148	0.26980
SF2	2	72.2567	0.35299	0.24960
TECB	2	73.1931	0.20471	0.14480
TPH	3	73.4035	0.04815	0.0278
VD	2	78.1711	0.78015	0.55170
VDF	2	62.9849	1.10966	0.78460

Additionally, RBCs with methacrylate-based matrices yielded statistically significant differences with respect to H, S, and EM, with methacrylate-based RBCs having greater stiffness, hardness, and elastic moduli values. These results were in contrast to another subsect of our study, which evaluated flexural strength (*FS*). It was determined that there was no statistically significant difference between *FS* and resin-matrix type in that study. Specifically, Admira Fusion (ORMOCER), Beautifil Bulk, Beautifil Bulk Flow, and Beautifil II (Giomers), GC Kalore (DX-511 monomer), and N'Durance (dimer acid) all were categorized as possessing non-methacrylate-based resin matrices. The chemistry of

Table 6: Filler Shape and Respective Mechanical Tests ($p<0.01$)

N is number of indents, S.D. is standard deviation, Std. Err.(x) is standard error of the mean

	N	Mean (x)	S.D.	Std. Err. (x)
Filler Shape	Stiffness (mN/m)			
Irregular	22632	1.49752	0.898971	0.00598
Regular	23352	0.96169	0.33358	0.00218
Filler Shape	Elastic Modulus (GPa)			
Irregular	22811	19.0552	7.13666	0.04725
Regular	23431	13.3968	3.54055	0.02313
Filler Shape	Hardness (GPa)			
Irregular	23567	60816.5	10027.6	65.32
Regular	23794	52849.8	7668.7	49.715

AF and N'D matrices have high molecular weights, which may lend themselves to lower polymerization shrinkage.[26] The giomer is a hybridization between resin composites and glass ionomers, and Beautifil composites specifically have surface-pre reacted glass ionomer (S-PRG) filler systems in which the silica filler is pre-treated with polyacrylic acid, free-dried, milled then silane-treated, and ground up before being added to the resin matrix.[27] While the variations in filler preparation and resin-type varied, non-methacrylate based resins performed poorer in the three mechanical properties- even with their filler weight percentages ranging from 69%-84%. This finding may suggest that irrespective of filler weight and/or loading, chemical interactions at the resin-filler interface may be responsible, in part, for a RBC's mechanical properties. This is also supported by the finding that due to differences in rigidity, crack propagation will usually initiate at the filler-matrix interface.[28]

Bivariate analysis was used to determine a correlation between filler weight percentage (see **Table 5** for wt% data) and *S*, *H*, and *EM*. *Figure 2* shows a positive, linear correlation for all three mechanical properties, with the greatest positive correlation

associated with *EM,* followed by *S,* and *H* having the lowest correlation to wt%. This linear correlation was also seen in other resin composites tested for effects of filler loading on elastic modulus and nanohardness,[16,29,30] as well as specifically in microfill composites with respect to stiffness and hardness.[31]

Results obtained by using laser particle diffraction from another subdivision of this study were used to classify filler distribution of each RBC tested. The particle diffraction yielded size versus frequency plots, which were used to interpret the filler size(s) with the highest frequency in a given RBC. If these plots had only one distinct peak, they were classified as "unimodal", indicating there was only one filler size in which the majority of filler particles in the sample presented with. If there were two distinct peaks, the composite was classified as "bimodal", and it was understood there were two distinct sizes of filler present at higher concentrations. Three or more peaks in the size/frequency curve indicated a sample had at least three (or more) distinct sizes of filler at greater concentrations. With certain exceptions, bimodal filler distribution had statistically significant higher values in S, H, and EM, than unimodal filler distribution. Multimodal filler distribution consistently was associated with the lowest values with respect to all three mechanical properties. These differences may be in part due to the amount of degree of conversion (DOC) of the RBC coupled with the size difference in filler distribution. It is possible that bimodal filler distribution may offer the strength accompanied with smaller, more densely packed filler agglomerates which are able to fill in the interstitial space between larger fillers, as well as the ability of increasing degree of conversion possible due to larger particle sizes interspersed within the resin matrix. However a due to complexities of DOC, consideration

of other characteristics such as resin-filler interface and matrix chemistry must be taken into consideration.[32,33]

Data from our study has not been analyzed in totality by statistical deconvolution, thus until all computations are complete, we may not speak upon the stiffness, hardness, and elastic modulus of RBCs tested as it pertains to the respective phases in each filler-matrix system. The aim of statistical deconvolution is to better characterize their phase micromechanical behaviors in hopes to relate each phase performance to macro mechanical properties (i.e. comparison to flexural strength, fracture toughness, and flexural fatigue degradation).

CONCLUSION

Composite systems adopted with new polymeric matrix chemistry behaved differently than methacrylate-based systems ($p<0.01$), although the differences in the behavior are still being investigated. Filler shape was also statistically significant, with irregular filler shape yielding larger values of elastic modulus, hardness, and stiffness. There were statistically significant differences between composite class types with respect to EM, H, S, as well as filler distribution. Based on the findings from this study, it may be recommended that when restoring in the posterior with resin-based composites, a nanohybrid composite with a methacrylate-based resin matrix, irregular filler shape, and bidomal filler distribution may perform best. However this is only a suggestion, as work is still being completed to statistically analyze and compare the results of the nanoscopic behaviors (i.e. EM, H, S) of the RBCs to their macromechanical features.

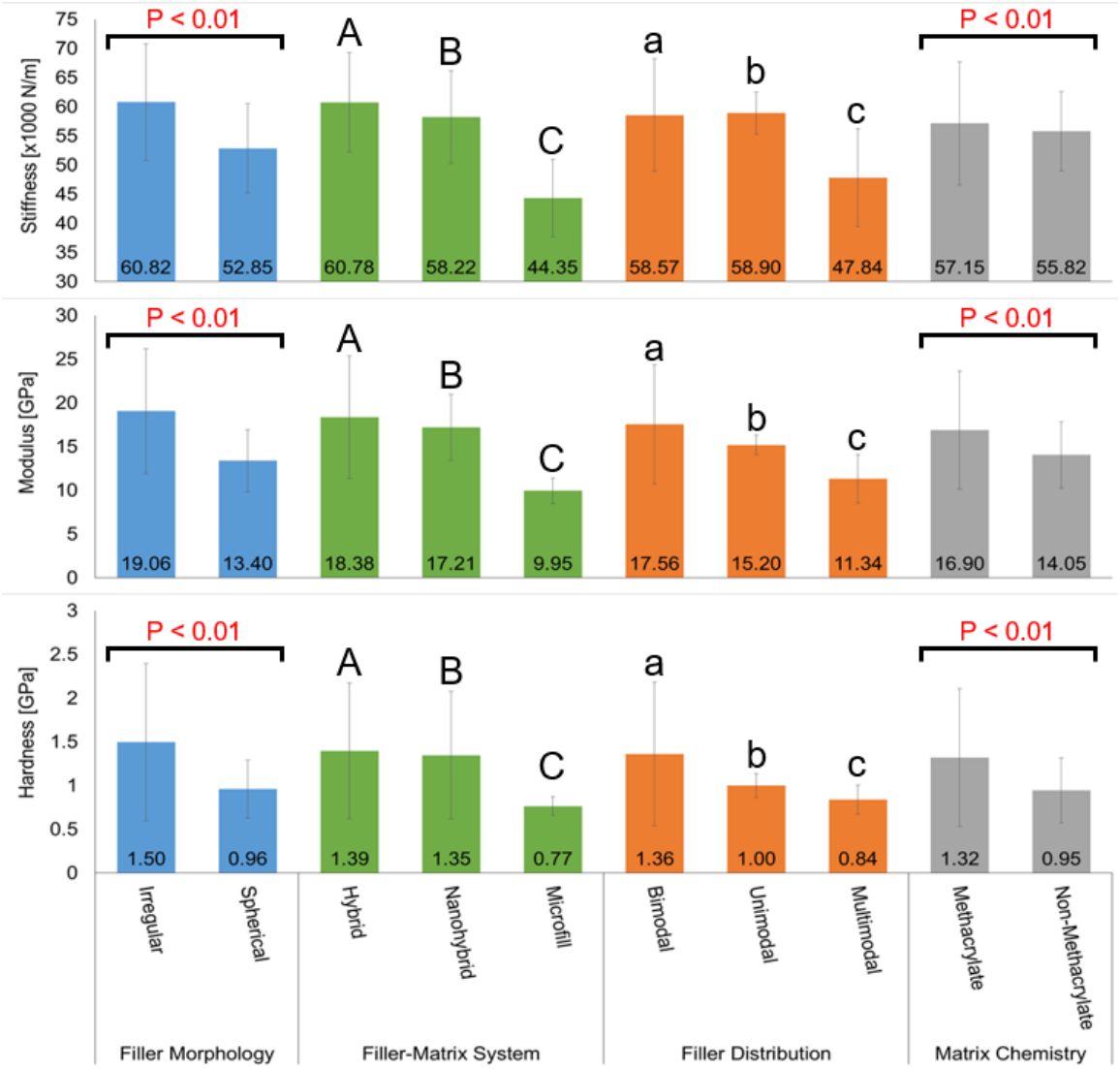

Figure 1. Effect of matrix chemistry and filler morphology, system, and distribution on hardness, elastic modulus, and stiffness. Columns with the same case letters are not statistically significant ($p > 0.01$).

.

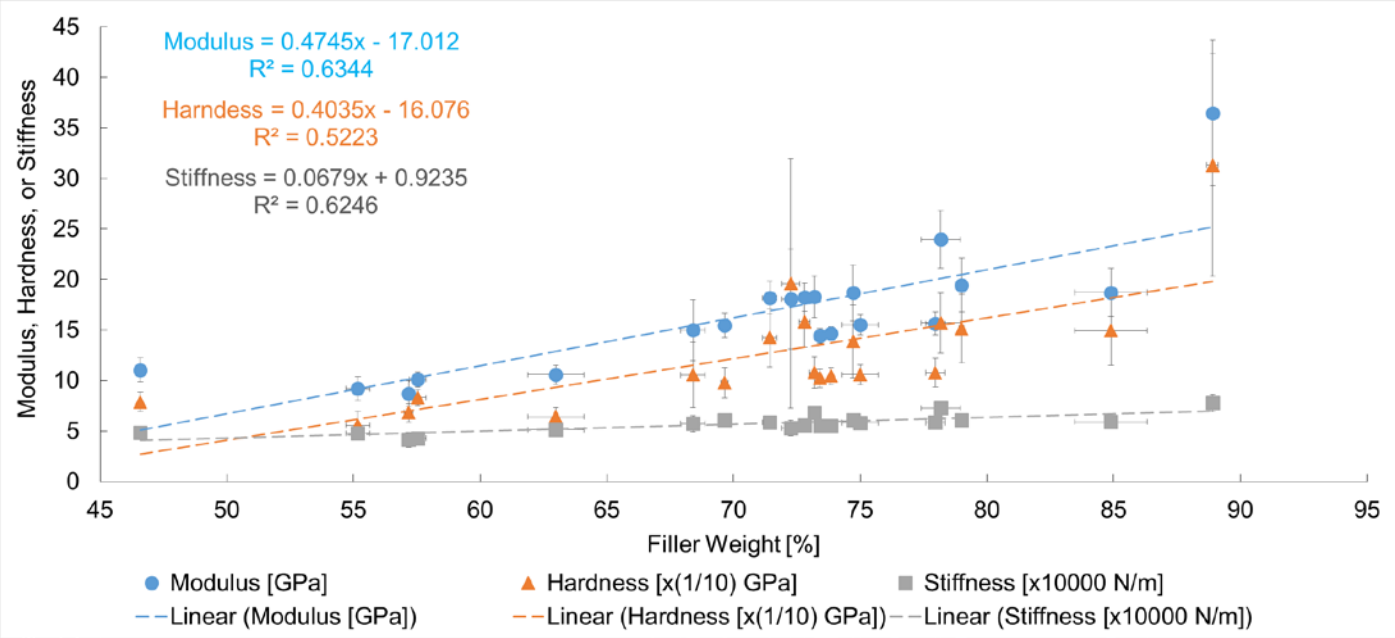

Figure 2. Modulus, hardness, or stiffness of various filler-matrix systems as a function of filler weight

REFERENCES

1. Opdam NJ, Bronkhorst EM, Roeters JM, Loomans BA. A retrospective clinical study on longevity of posterior composite and amalgam restorations. Dent Mater. 2007; 23(1): 2-8.

2. Naghipur S, Pesun I, Nowakowski A, Kim A. Twelve-year survival of 2-surface composite resin and amalgam premolar restorations placed by dental students. J Prosthet Dent. 2016; 116 (3): 336-339.

3. Rho YJ, Namgung C, Jin BH, Lim BS, Cho BH. Longevity of direct restorations in stress-bearing posterior cavities: a retrospective study. Oper Dent. 2013; 38 (2013): 572-582.

4. Beck F, Lettner S, Graf A, Bitriol B, Dumitrescu N, Bauer P, Moritz A, Schedle A. Survival of direct resin restorations in posterior teeth within a 19-year period (1996–2015): A meta-analysis of prospective studies. Dent Mater. 2015;31(8): 958-985.

5. Brunthaler A, Konig F, Lucas T, Sperr W, Schedle A. Longevity of direct resin composite restorations in posterior teeth. Clin Oral Investig. 2003; 7(2) 63–70.

6. Sarrett, D.C. Clinical challenges and the relevance of materials testing for posterior composite restorations. Dent Mater. 2005; 21: 9-20.

7. Anusavice, K.J., Shen, C., Rawls, H.R. Phillips' science of dental materials. Elsevier Health Sciences, 2013.

8. Randolph, L. D., Palin, W. M., Leloup, G., & Leprince, J. G. (2016). Filler characteristics of modern dental resin composites and their influence on physico-mechanical properties. Dental Materials, 32(12), 1586-1599.

9. Lohbauer, U., Frankenberger, R., Krämer, N., & Petschelt, A. (2006). Strength and fatigue performance versus filler fraction of different types of direct dental restoratives. Journal of Biomedical Materials Research Part B: Applied Biomaterials: An Official Journal of The Society for Biomaterials, The Japanese Society for Biomaterials, and The Australian Society for Biomaterials and the Korean Society for Biomaterials, 76(1), 114-120.

10. Willems, G., Lambrechts, P., Braem, M., & Vanherle, G. (1993). Three-year follow-up of five posterior composites: in vivo wear. Journal of dentistry, 21(2), 74-78.

11. Abe Y, Lambrechts P, Inoue S, Braem MJA, Takeuchi M, Vanherle G, Van Meerbeek B. Dynamic elastic modulus of 'packable' composites. Dent Mater. 2001; 17(6) 520-525.

12. Sabbagh, J., Vreven, J., & Leloup, G. (2002). Dynamic and static moduli of elasticity of resin-based materials. Dental Materials, 18(1), 64-71.

13. Nakayama, W. T., Hall, D. R., Grenoble, D. E., & Katz, J. L. (1974). Elastic properties of dental resin restorative materials. Journal of dental research, 53(5), 1121-1126.

14. Lohbauer U, Beli R, Ferracane JL, Factors Involved in Mechanical Fatigue Degradation of Dental Resin Composites. J Dent Res. 2013; 92(7): 584-591.

15. Lakes, R. Materials with structural hierarchy. Nature. 1993; 361: 511-515.

16. Masouras K, Riaz A, Watts DC, Silikas, N. Effect of filler size and shape on local nanoindentation modulus of resin-composites. J Mater Sci Mater Med. 2008; 19(12): 3561–3566.

17. Oliver, W. C., & Pharr, G. M. (1992). An improved technique for determining hardness and elastic modulus using load and displacement sensing indentation experiments. Journal of materials research, 7(6), 1564-1583.

18. Qian, L., Li, M., Zhou, Z., Yang, H., & Shi, X. (2005). Comparison of nano-indentation hardness to microhardness. Surface and Coatings Technology, 195(2-3), 264-271.

19. Ferracane, J. L. (2013). Resin-based composite performance: are there some things we can't predict?. Dental materials, 29(1), 51-58.

20. Dewaele, M., Truffier-Boutry, D., Devaux, J., & Leloup, G. (2006). Volume contraction in photocured dental resins: the shrinkage-conversion relationship revisited. Dental Materials, 22(4), 359-365.

21. Kleverlaan, C. J., & Feilzer, A. J. (2005). Polymerization shrinkage and contraction stress of dental resin composites. Dental Materials, 21(12), 1150-1157.

22. Constantinides, G., & Ulm, F. J. (2007). The nanogranular nature of C–S–H. Journal of the Mechanics and Physics of Solids, 55(1), 64-90.

23. ISO, S. 14577-1: 2015. Metallic materials-Instrumented indentation test for hardness and materials parameters-Part, 1.

24. Moraes, R. R., Goncalves, L. D. S., Lancellotti, A. C., Consani, S., Correr-Sobrinho, L., & Sinhoreti, M. A. (2009). Nanohybrid resin composites: nanofiller loaded materials or traditional microhybrid resins?. Operative dentistry, 34(5), 551-557.

25. Kim, K. H., Ong, J. L., & Okuno, O. (2002). The effect of filler loading and morphology on the mechanical properties of contemporary composites. The Journal of prosthetic dentistry, 87(6), 642-649.

26. Ferracane, J. L. (2011). Resin composite—state of the art. Dental materials, 27(1), 29-38.

27. Sunico, M. C., Shinkai, K., & Katoh, Y. (2005). Two-year clinical performance of occlusal and cervical giomer restorations. OPERATIVE DENTISTRY-UNIVERSITY OF WASHINGTON-, 30(3), 282.

28. Tanimoto, Y., Nishiwaki, T., Nemoto, K., & Ben, G. (2004). Effect of filler content on bending properties of dental composites: Numerical simulation with the use of the finite - element method. Journal of Biomedical Materials Research Part B: Applied Biomaterials: An Official Journal of The Society for Biomaterials, The Japanese Society for Biomaterials, and The Australian Society for Biomaterials and the Korean Society for Biomaterials, 71(1), 188-195.

29. El-Safty, S., Akhtar, R., Silikas, N., & Watts, D. C. (2012). Nanomechanical properties of dental resin-composites. Dental Materials, 28(12), 1292-1300.

30. Ilie, N., Bucuta, S., & Draenert, M. (2013). Bulk-fill resin-based composites: an in vitro assessment of their mechanical performance. Operative dentistry, 38(6), 618-625.

31. Germain, H. S., Swartz, M. L., Phillips, R. W., Moore, B. K., & Roberts, T. A. (1985). Properties of microfilled composite resins as influenced by filler content. Journal of Dental Research, 64(2), 155-160.

32. Turssi, C. P., Ferracane, J. L., & Vogel, K. (2005). Filler features and their effects on wear and degree of conversion of particulate dental resin composites. Biomaterials, 26(24), 4932-4937.

33. Hong, J., Yoon, S., Hwang, T., Oh, J., Lee, Y., & Nam, J. (2011). Effect of Filler Size and its Bimodal Distribution for Highly Thermal-Conductive Epoxy Composites. In 18th International Conference on Composite Materials (poster presentation), Suwon, South Korea.